Electroweak radiative corrections to $e^+e^- \to t\bar{t}H$

A. Denner [a], S. Dittmaier [b], M. Roth [c], M.M. Weber [a]

[a] *Paul Scherrer Institut, Würenlingen und Villigen, CH-5232 Villigen PSI, Switzerland*
[b] *Max-Planck-Institut für Physik (Werner-Heisenberg-Institut), D-80805 München, Germany*
[c] *Institut für Theoretische Physik, Universität Karlsruhe, D-76128 Karlsruhe, Germany*

Abstract

We have calculated the complete electroweak $\mathcal{O}(\alpha)$ radiative corrections to the Higgs-boson production process $e^+e^- \to t\bar{t}H$ in the electroweak Standard Model. Initial-state radiation beyond $\mathcal{O}(\alpha)$ is included in the structure-function approach. The calculation of the corrections is briefly described, and numerical results are presented for the total cross section. Both the photonic and the genuine weak corrections reach the order of about 10% or even more and show a non-trivial dependence on the Higgs-boson mass and on the scattering energy. We compare our results with two previous calculations that obtained differing results at high energies.

© 2003 Elsevier B.V. Open access under CC BY license.

1. Introduction

In the electroweak Standard Model (SM) all fermions f receive their masses m_f via Yukawa couplings to the Higgs field. Splitting the Higgs field into its vacuum-expectation value $v = (\sqrt{2}\,G_\mu)^{-1/2} \approx$ 246 GeV and the physical excitation $H(x)$, the Yukawa term in the SM Lagrangian reads $\mathcal{L}_{\text{Yuk}} = -\sum_f m_f (1 + H(x)/v)\bar{\psi}_f \psi_f$. Thus, the Yukawa coupling strength is predicted to be m_f/v at tree level, and the experimental determination of the Higgs-fermion couplings represents an important test of the mass generation via the Higgs mechanism. Since the top quark is the heaviest of all fermions, it is supposed to play a key role in a theory of fermion masses. Therefore,

the measurement of the top-quark Yukawa coupling is of particular interest. For not too large Higgs-boson masses, $M_H \sim 100$–200 GeV, a promising process for this task is $e^+e^- \to t\bar{t}H$, as already pointed out in Ref. [1]. To achieve a measurement with a precision of the order of $\sim 5\%$, however, an e^+e^- linear collider (LC) with high centre-of-mass (CM) energies ($\sqrt{s} \sim$ 800–1000 GeV) and high luminosity ($L \sim 1000\,\text{fb}^{-1}$) is required [2]. A better accuracy might be obtained by a simultaneous fit of various Higgs-boson parameters to the whole profile of the Higgs boson at a LC [3]. Moreover, an investigation of the process $e^+e^- \to t\bar{t}H$ might be useful for setting bounds on non-standard physics [1,4] in the top-quark–Higgs-boson coupling.

A determination of the top-quark Yukawa coupling at the level of a few per-cent requires both a proper understanding of the background [5] to the decaying $t\bar{t}H$ final state and a theoretical prediction of the

E-mail address: ansgar.denner@psi.ch (A. Denner).

$e^+e^- \to t\bar{t}H$ signal cross section within per-cent accuracy. Thus, radiative corrections have to be controlled within this accuracy, a task that is rather complicated for a process with three massive unstable particles in the final state. As a first step, the process $e^+e^- \to t\bar{t}H$ can be treated in the approximation of stable top quarks and Higgs bosons in the final state. The corresponding lowest-order predictions are already known for a long time [6]. These results were supplemented by the $\mathcal{O}(\alpha_s)$ QCD corrections to the total production cross section in the SM, first within the "effective Higgs-boson approximation" [7] that is valid only for small Higgs-boson masses and very high energies, and subsequently [8,9][1] based on the full set of QCD diagrams in $\mathcal{O}(\alpha_s)$. The QCD corrections to Higgs-boson production in association with heavy-quark pairs ($t\bar{t}/b\bar{b}$) in the minimal supersymmetric SM were discussed in Refs. [10–12].[2] Besides corrections to total cross sections, the QCD corrections to the Higgs-boson energy distribution were discussed in Ref. [13], both for the SM and its minimal supersymmetric extension. Recently first results for the electroweak $\mathcal{O}(\alpha)$ corrections to $e^+e^- \to t\bar{t}H$ in the SM have been presented in Refs. [14] and [15]. These calculations were found to agree for small energies but to differ at high energies.

In this Letter we present results of a further, completely independent calculation of the $\mathcal{O}(\alpha)$ electroweak corrections, which is additionally improved by the leading higher-order corrections from initial-state radiation. Details on this calculation, which we have also implemented in a Monte Carlo event generator, will be given elsewhere. Here we sketch only the main ingredients. Moreover, we compare our results with those of Refs. [14,15]. While we find good agreement with the results of the recent calculation of Ref. [15] at all considered energies, our results differ from those of Ref. [14] at high energies and close to threshold. Moreover, we could reproduce the QCD

corrections of Ref. [8] from our results on photonic final-state radiation within statistical integration errors.

2. Method of calculation

We have calculated the complete $\mathcal{O}(\alpha)$ electroweak virtual and real photonic corrections to the process $e^+e^- \to t\bar{t}H$, following the same strategy as used in our previous calculation of the corrections to $e^+e^- \to \nu\bar{\nu}H$ [16].

The calculation of the one-loop diagrams has been performed in the 't Hooft–Feynman gauge both in the conventional and in the background-field formalism using the conventions of Refs. [17,18], respectively. The renormalization is carried out in the on-shell renormalization scheme, as described there. The electron mass m_e is neglected whenever possible.

The calculation of the Feynman diagrams has been performed in two completely independent ways, leading to two independent computer codes for the numerical evaluation. Both calculations are based on the methods described in Ref. [17]. Apart from the 5-point functions the tensor coefficients of the one-loop integrals are recursively reduced to scalar integrals with the Passarino–Veltman algorithm [19] at the numerical level. The scalar integrals are evaluated using the methods and results of Refs. [17,20], where ultraviolet divergences are regulated dimensionally and IR divergences with an infinitesimal photon mass. The 5-point functions are reduced to 4-point functions following Ref. [21], where a method for a direct reduction is described that avoids leading inverse Gram determinants which potentially cause numerical instabilities. The two calculations differ in the following points. In the first calculation, the Feynman graphs are generated with FEYNARTS version 1.0 [22]. Using MATHEMATICA the amplitudes are expressed in terms of standard matrix elements and coefficients of tensor integrals. The whole calculation has been carried out in the conventional and in the background-field formalism. The second calculation has been done with the help of FEYNARTS version 3 [23], and the analytical expressions have been generated by FORMCALC [24] and translated into a C code. The scalar and tensor coefficients, in particular those for the 5-point functions,

---

[1] In Ref. [9] only the QCD corrections to the photon-exchange channel for $t\bar{t}H$ production were taken into account.

[2] In Ref. [10] only the photon-exchange channel is corrected, so that the relative correction given there coincides with the one obtained in Ref. [9] where the SM process is treated analogously. The calculation of Ref. [11] includes the full set of $\mathcal{O}(\alpha_s)$ QCD diagrams, and in Ref. [12] the SUSY-QCD corrections to $e^+e^- \to t\bar{t}H$ are considered.

have been evaluated by own routines, as described above.

The results of the two different codes, and also those obtained within the conventional and background-field formalism, are in good numerical agreement (typically within at least 12 digits for non-exceptional phase-space points and double precision). The agreement of the results in the conventional and background-field formalism, in particular, checks the gauge independence of our results.

The matrix elements for the real photonic corrections are evaluated using the Weyl–van der Waerden spinor technique as formulated in Ref. [25] and have been successfully checked against the result obtained with the package MADGRAPH [26]. The soft and collinear singularities are treated in the dipole subtraction method [27]. Beyond $\mathcal{O}(\alpha)$ initial-state-radiation (ISR) corrections are included at the leading-logarithmic level using the structure functions given in Ref. [28] (for the original papers see references therein).

The phase-space integration is performed with Monte Carlo techniques in both computer codes. The first code employs a multi-channel Monte Carlo generator similar to the one implemented in RACOONWW [29,30] and LUSIFER [31], the second one uses the adaptive multi-dimensional integration program VE-GAS [32].

3. Numerical results

For the numerical evaluation we use the following set of SM parameters [33],

$$G_\mu = 1.16639 \times 10^{-5} \text{ GeV}^{-2},$$

$$\alpha(0) = 1/137.03599976, \quad \alpha_s(M_Z) = 0.1172,$$

$$M_W = 80.423 \text{ GeV}, \quad M_Z = 91.1876 \text{ GeV},$$

$$m_e = 0.510998902 \text{ MeV}, \quad m_\mu = 105.658357 \text{ MeV},$$

$$m_\tau = 1.77699 \text{ GeV}, \quad m_u = 66 \text{ MeV},$$

$$m_c = 1.2 \text{ GeV}, \quad m_t = 174.3 \text{ GeV},$$

$$m_d = 66 \text{ MeV}, \quad m_s = 150 \text{ MeV},$$

$$m_b = 4.3 \text{ GeV}. \tag{3.1}$$

We do not calculate the W-boson mass from G_μ but use its experimental value as input. The masses of the light quarks are adjusted to reproduce the hadronic contribution to the photonic vacuum polarization of Ref. [34]. We parametrize the lowest-order cross section with the Fermi constant G_μ (G_μ-scheme), i.e., we derive the electromagnetic coupling α according to $\alpha_{G_\mu} = \sqrt{2}\, G_\mu M_W^2 s_W^2/\pi$. This, in particular, absorbs the running of the electromagnetic coupling $\alpha(Q^2)$ from $Q = 0$ to the electroweak scale ($Q \sim M_Z$) into the lowest-order cross section so that the results are practically independent of the masses of the light quarks. In the relative radiative corrections, we use, however, $\alpha(0)$ as coupling parameter, which is the correct effective coupling for real photon emission.

In the following we separate the *photonic* corrections, which comprise loop diagrams with virtual photon exchange in the loop and the corresponding parts of the counter terms as well as real photon emission, from the full electroweak $\mathcal{O}(\alpha)$ corrections; the remaining non-photonic electroweak corrections are called *weak*. Since the lowest-order diagrams involve only neutral-current couplings, but no W-boson exchange, this splitting is gauge invariant. Moreover, we separately discuss the *higher-order* (i.e., beyond $\mathcal{O}(\alpha)$) *ISR* corrections that are obtained from the convolution of the lowest-order cross section with the leading-logarithmic structure functions, but with the $\mathcal{O}(\alpha)$ contribution subtracted. The higher-order ISR is included in the electroweak corrections shown in the following plots.

In addition to the electroweak corrections, we also include results on the QCD corrections which can be deduced from the part of the photonic corrections that is proportional to Q_t^2, where $Q_t = 2/3$ is the relative electric charge of the top quark, i.e., from the final-state radiation (FSR). The QCD correction is obtained from these corrections upon replacing the factor $Q_t^2 \alpha$ by $C_F \alpha_s = 4\alpha_s(\mu^2)/3$. Following Ref. [8], the QCD renormalization scale μ is set to the CM energy in the following, and the running of the strong coupling is evaluated at the two-loop level ($\overline{\text{MS}}$ scheme) with five active flavours, normalized by $\alpha_s(M_Z^2)$ as given in Eq. (3.1). For $\sqrt{s} = 500, 800,$ and 1000 GeV the resulting values for the strong coupling are given by $\alpha_s(M_Z^2) = 0.09349, 0.08857,$ and 0.08642, respectively.

In this Letter, we consider merely total cross sections without any cuts; distributions will be discussed elsewhere. For reference we give some numbers for

Table 1
Lowest-order cross section for $e^+e^- \to t\bar{t}H$ in the G_μ-scheme, σ_{tree}, cross section including electroweak and QCD corrections, σ_{corr}, and various contributions to the relative corrections δ (as described in the text) for various Higgs-boson masses at $\sqrt{s} = 500$, 800 GeV, and 1 TeV

$\sqrt{s} = 500$ GeV	M_H [GeV]		
	115	125	140
σ_{tree} [fb]	0.47901(7)	0.23150(3)	0.038189(6)
σ_{corr} [fb]	0.6506(6)	0.3401(4)	0.0713(1)
δ_{QCD} [%]	46.5(1)	59.2(2)	103.4(3)
δ_{phot} [%]	−30.64(1)	−34.69(1)	−44.51(1)
δ_{hoISR} [%]	4.25(3)	5.53(3)	9.28(3)
δ_{weak} [%]	15.70(3)	16.85(3)	18.51(3)

$\sqrt{s} = 800$ GeV	M_H [GeV]					
	115	150	200	250	300	350
σ_{tree} [fb]	2.7004(4)	1.7406(3)	0.9217(1)	0.46076(6)	0.20432(3)	0.07165(1)
σ_{corr} [fb]	2.541(1)	1.6076(7)	0.8443(4)	0.4251(2)	0.1904(1)	0.06648(6)
δ_{QCD} [%]	−0.87(2)	0.36(3)	2.43(4)	5.03(4)	8.58(6)	14.12(6)
δ_{phot} [%]	−5.30(1)	−8.26(1)	−12.54(1)	−16.76(1)	−21.54(1)	−27.55(1)
δ_{hoISR} [%]	−0.41(3)	−0.19(3)	0.22(3)	0.79(3)	1.59(3)	2.86(3)
δ_{weak} [%]	0.69(1)	0.45(1)	1.49(1)	3.19(1)	4.56(1)	3.36(5)

$\sqrt{s} = 1000$ GeV	M_H [GeV]					
	115	150	200	250	300	350
σ_{tree} [fb]	2.2594(3)	1.6208(2)	1.0356(2)	0.6643(1)	0.41894(6)	0.25510(4)
σ_{corr} [fb]	2.061(1)	1.4311(7)	0.8900(5)	0.5639(3)	0.3510(2)	0.2045(2)
δ_{QCD} [%]	−4.76(2)	−4.37(2)	−3.72(3)	−2.99(3)	−2.26(4)	−1.73(5)
δ_{phot} [%]	−0.34(1)	−2.89(1)	−6.35(1)	−9.41(1)	−12.43(1)	−15.55(1)
δ_{hoISR} [%]	−0.61(3)	−0.52(3)	−0.34(3)	−0.11(3)	0.19(3)	0.57(3)
δ_{weak} [%]	−3.06(2)	−3.91(2)	−3.66(3)	−2.61(2)	−1.71(2)	−3.13(3)

the total cross section in lowest order, σ_{tree}, the cross section including electroweak and QCD corrections, σ_{corr}, and the various contributions to the relative corrections defined as $\delta = \sigma/\sigma_{tree} - 1$ in Table 1. The last numbers in parentheses correspond to the Monte Carlo integration error of the last given digits. In Figs. 1–3 we show the lowest-order cross section as well as the corresponding corrections as a function of the Higgs-boson mass for the typical LC CM energies $\sqrt{s} = 500$, 800 GeV, and 1 TeV. In Figs. 4–6 the results are illustrated for fixed Higgs-boson masses of $M_H = 115$, 150, and 200 GeV.

Away from the kinematic threshold at $\sqrt{s} = 2m_t + M_H$ the total cross section is typically of the order of 0.5–3 fb and becomes maximal in the energy range between 700 GeV and 1 TeV for small Higgs-boson masses. As already discussed in Refs. [8,9] in detail, the QCD corrections are positive and rather large in the threshold region ($\sqrt{s} \gtrsim 2m_t + M_H$), where soft-gluon exchange between in the $t\bar{t}$ system leads to a

Coulomb-like singularity. Away from threshold this singularity is diluted by the larger phase space, since the singularity demands a low relative velocity of the quarks. Averaging the singular factor over the phase space leads to the following threshold behaviour of the QCD correction [8],

$$\delta_{QCD} \sim \frac{32\alpha_s}{9\beta_t}, \qquad \delta_{FSR} \sim \frac{8Q_t^2\alpha}{3\beta_t},$$

$$\beta_t = \frac{\sqrt{(\sqrt{s} - M_H)^2 - 4m_t^2}}{2m_t}, \qquad (3.2)$$

where β_t is the maximal quark velocity in the $t\bar{t}$ rest frame. The FSR corrections show the same behaviour,[3] however, suppressed by the factor $Q_t^2\alpha/(4\alpha_s/3) \sim 0.02$. Although the relative QCD correction becomes rather huge close to threshold, it should be real-

---

[3] Because of the dominance of the ISR corrections this is not visible in the following figures.
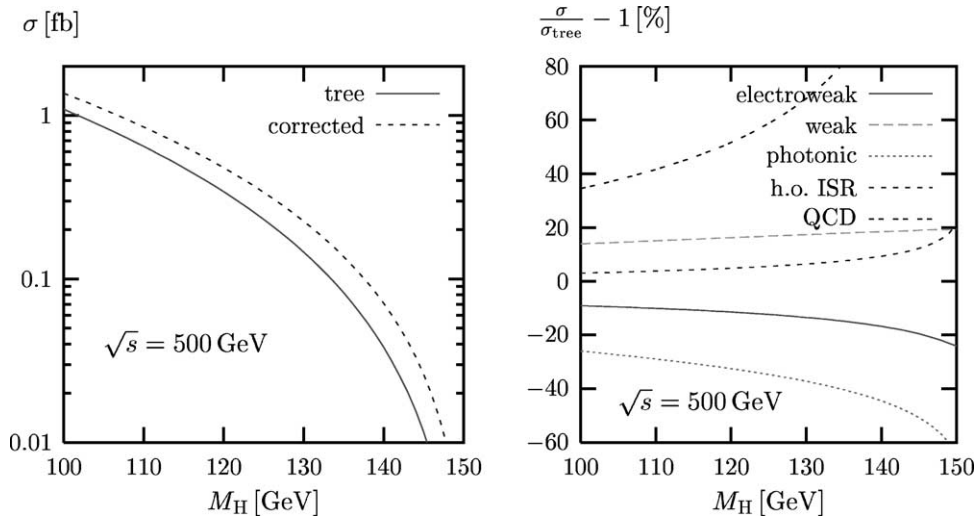
Fig. 1. Lowest-order and corrected cross sections (l.h.s.) as well as relative corrections (r.h.s.) in the G_μ-scheme for a CM energy $\sqrt{s} = 500$ GeV.
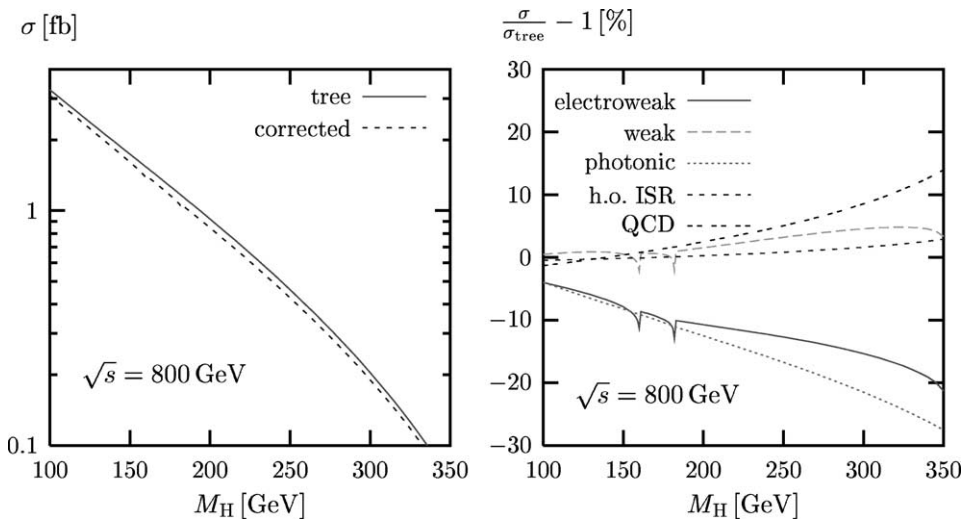

Fig. 2. Lowest-order and corrected cross sections (l.h.s.) as well as relative corrections (r.h.s.) in the G_μ-scheme for a CM energy $\sqrt{s} = 800$ GeV.

ized that the total cross section decreases rapidly there. In the region above threshold, where the cross section is largest, the QCD correction is only of the order of a per-cent. For CM energies and Higgs-boson masses far above threshold, the QCD corrections even turn negative and reduce the cross section by about 5% at $\sqrt{s} = 1$ TeV. This behaviour is expected from the effective Higgs-boson approximation [7], as also argued in Ref. [8].

The photonic corrections are negative for CM energies below 1 TeV and not too small Higgs-boson masses, i.e., not too far away from threshold. This is due to large virtual photonic corrections which are not cancelled by the corresponding real radiation owing to the decreasing phase-space volume for real-photon emission with increasing M_H or decreasing $\sqrt{s}$. Therefore, the photonic corrections are large and negative, in particular, at the relatively small scattering
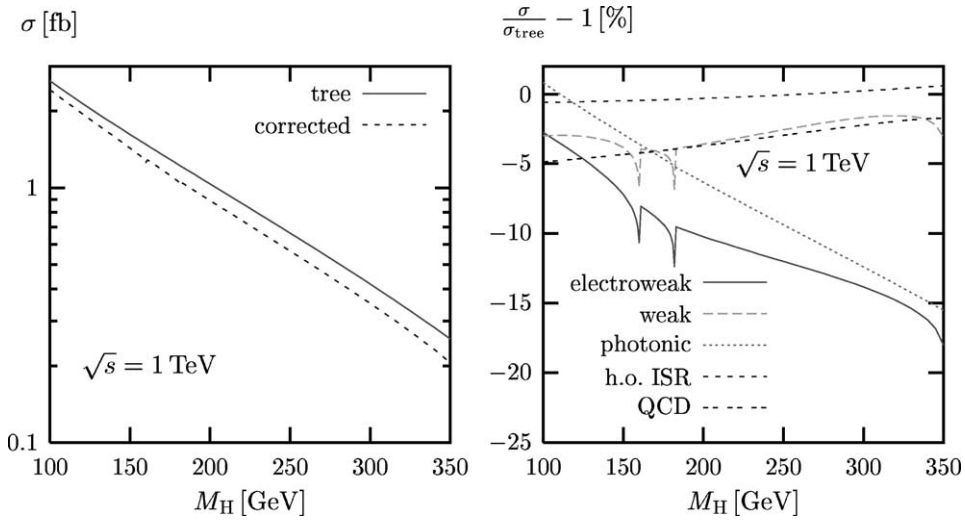
Fig. 3. Lowest-order and corrected cross sections (l.h.s.) as well as relative corrections (r.h.s.) in the G_μ-scheme for a CM energy $\sqrt{s} = 1$ TeV.
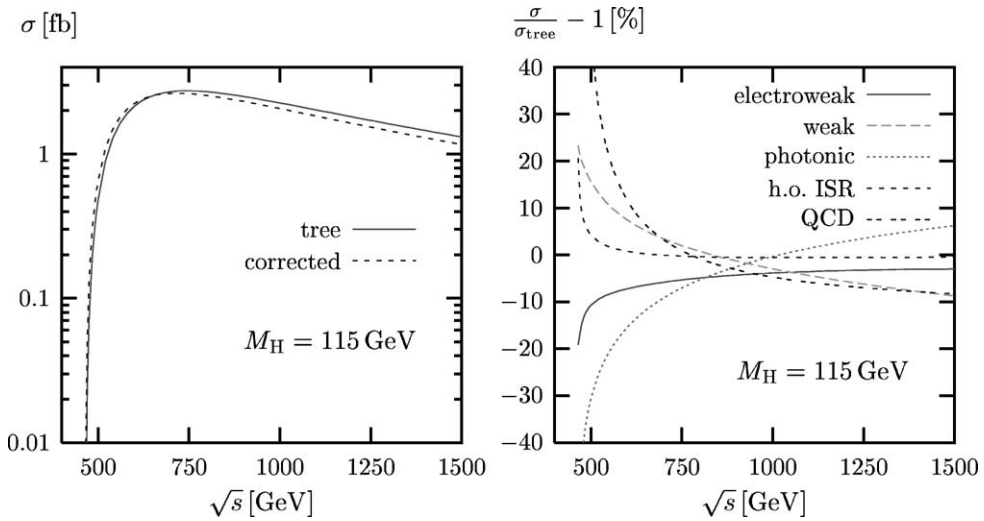

Fig. 4. Lowest-order and corrected cross sections (l.h.s.) as well as relative corrections (r.h.s.) in the G_μ-scheme for a Higgs-boson mass $M_H = 115$ GeV.

energy of $\sqrt{s} = 500$ GeV, where they reach -25 to -65% for $M_H = 100$–150 GeV. In this situation resummation of the large photonic corrections is mandatory. The bulk of these contributions is included in our calculation (higher-order ISR) and for $\sqrt{s} = 500$ GeV amounts to 3–20%. Away from threshold, the photonic $\mathcal{O}(\alpha)$ corrections grow with increasing $\sqrt{s}$ and reach $+7\%$ for $M_H = 115$ GeV and $\sqrt{s} = 1.5$ TeV.

The higher-order ISR stays below 1% for $\sqrt{s}$ at least 150 GeV above threshold.

The genuine weak corrections strongly depend on the scattering energy, while the dependence on the Higgs-boson mass is moderate. For $\sqrt{s} = 500$ GeV they are about 15–20%, i.e., large and positive. For increasing CM energy they decrease and are at the per-cent level around $\sqrt{s} \sim 800$ GeV. For TeV energies
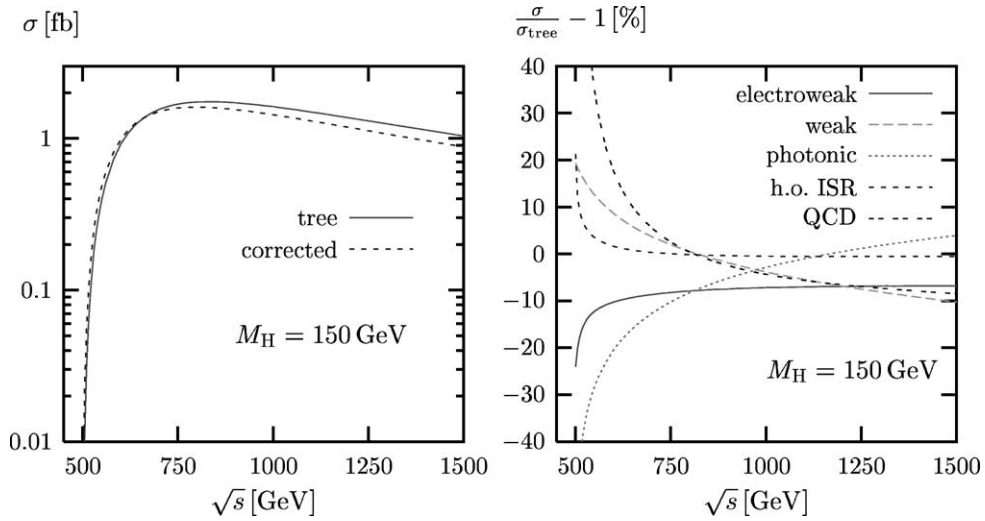
Fig. 5. Lowest-order and corrected cross sections (l.h.s.) as well as relative corrections (r.h.s.) in the G_μ-scheme for a Higgs-boson mass $M_H = 150$ GeV.
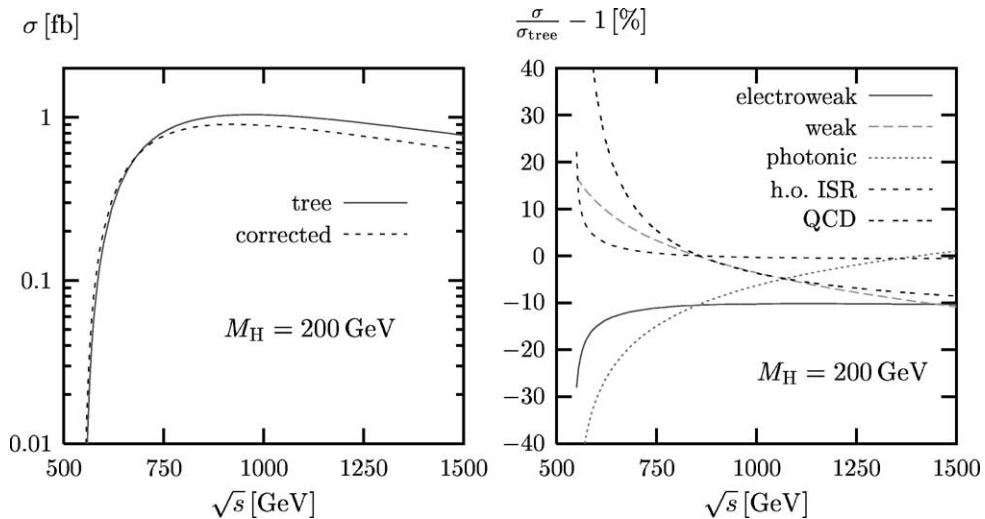

Fig. 6. Lowest-order and corrected cross sections (l.h.s.) as well as relative corrections (r.h.s.) in the G_μ-scheme for a Higgs-boson mass $M_H = 200$ GeV.

they become more and more negative and reach the order of -10% around 1.5 TeV. While the weak corrections are smaller than the QCD corrections in the threshold region, both contributions are of similar size about 250 GeV above threshold, i.e., near the peak of the cross section. At high energies the size of the weak corrections grows faster than the one of the QCD corrections. Such a behaviour is typical if Sudakov logarithms like $\alpha \ln^2(s/M_W^2)$ dominate the

weak corrections at high energies. Note that we use the G_μ-scheme, and that the weak corrections are shifted by $\sim \pm 10\%$ when transformed to other schemes like the $\alpha(0)$ or the $\alpha(s)$ schemes (see also Ref. [16]). The spikes at $M_H = 2M_W, 2M_Z$ result from thresholds and are well known from the process $e^+e^- \to ZH$ [35].

Photonic and weak corrections partially cancel each other, and the resulting electroweak corrections increase very weakly with $\sqrt{s}$ apart from the region

Table 2

Total cross section in lowest order and including the full electroweak $\mathcal{O}(\alpha)$ corrections as well as the relative corrections for various CM energies and Higgs-boson masses for the input-parameter scheme of Ref. [14]. The statistical errors of Ref. [14] are estimated by the authors to be below 1% (cf. Footnote 4)

$\sqrt{s}$ [GeV]	M_H [GeV]	σ_{tree} [fb]	$\sigma_{\mathcal{O}(\alpha)}$ [fb]	δ_{ew} [%]	
500	115	0.43343	0.4173	−4.26	Ref. [14]
	115	0.43341(6)	0.4150(2)	−4.25(5)	this work
500	150	4.8142×10^{-4}	3.401×10^{-4}	−29.35	Ref. [14]
	150	$4.8140(8) \times 10^{-4}$	$3.168(4) \times 10^{-4}$	−34.19(8)	this work
600	200	0.15359	0.1439	−6.34	Ref. [14]
	200	0.15359(2)	0.14194(7)	−7.58(4)	this work
800	115	2.44	2.60	6.52	Ref. [14]
	115	2.4434(3)	2.5913(7)	6.06(2)	this work
800	150	1.58	1.63	3.60	Ref. [14]
	150	1.5749(2)	1.6243(4)	3.14(2)	this work
800	200	0.8341	0.8454	1.36	Ref. [14]
	200	0.8340(1)	0.8357(2)	0.21(2)	this work
1000	115	2.04	2.19	7.29	Ref. [14]
	115	2.0443(3)	2.1935(5)	7.30(2)	this work
1000	150	1.47	1.53	4.47	Ref. [14]
	150	1.4664(2)	1.5273(4)	4.15(2)	this work
1000	200	0.9372	0.9567	2.09	Ref. [14]
	200	0.9370(1)	0.9492(2)	1.29(2)	this work
2000	115	0.7614	0.7919	4.02	Ref. [14]
	115	0.7613(1)	0.8214(4)	7.90(5)	this work
2000	150	0.6270	0.6297	0.43	Ref. [14]
	150	0.6269(1)	0.6526(3)	4.11(5)	this work
2000	200	0.4968	0.4790	−3.55	Ref. [14]
	200	0.49659(8)	0.5003(3)	0.74(5)	this work

close to threshold, where the electroweak corrections decrease fast with decreasing $\sqrt{s}$ and reach of the order of −20% at threshold. Away from threshold, they are at the level of −5, −8, and −11% for $M_H = 115$, 150, and 200 GeV, respectively, and thus become increasingly negative with increasing Higgs-boson mass.

4. Comparison with other calculations

The results on the QCD corrections given in Table 1 have been reproduced with the (publically available) computer code based on the calculation of Ref. [8]. We found agreement within the statistical integration errors.

For a comparison of the electroweak $\mathcal{O}(\alpha)$ corrections with the results of Ref. [14] we changed our in-put parameters to the ones quoted there and switched to the $\alpha(0)$-scheme, where G_μ is ignored in the input and all couplings are deduced from $\alpha(0)$. In Table 2 we compare some representative numbers [4] from the calculation of Ref. [14] with the corresponding results from our Monte Carlo generator. The numbers in parentheses give the errors in the last digits of our calculation. The tree-level cross sections coincide within 0.03%. Most of the numbers for the one-loop corrected cross sections agree within 1–2%, i.e., roughly within the estimated error of Ref. [14]. However, for the corrected cross sections at $\sqrt{s} = 2$ TeV, i.e., at high energies, and the one very close to threshold, i.e., for $\sqrt{s} = 500$ GeV and $M_H = 150$ GeV, we find differences of 4 and 7%, respectively. The same holds for

---

[4] These numbers were kindly provided to us by Zhang Ren-You and You Yu quoting a statistical error below 1%.

Table 3
Total cross section in lowest order and including the full electroweak $\mathcal{O}(\alpha)$ corrections as well as the relative electroweak, weak, and photonic corrections for various CM energies and Higgs-boson masses for the input-parameter scheme of Ref. [15]

$\sqrt{s}$ [GeV]	M_H [GeV]	σ_{tree} [fb]	$\sigma_{\mathcal{O}(\alpha)}$ [fb]	δ_{ew} [%]	δ_{weak} [%]	δ_{phot} [%]	
600	120	1.7293(3)	1.738(2)	0.5	16.5	−16.0	Ref. [15]
	120	1.7292(2)	1.7368(6)	0.44(3)	16.49(3)	−16.03(1)	this work
600	180	0.33714(4)	0.3126(3)	−7.3	18.4	−25.7	Ref. [15]
	180	0.33714(5)	0.3124(1)	−7.34(3)	18.38(3)	−25.72(1)	this work
800	120	2.2724(5)	2.362(4)	3.9	9.5	−5.6	Ref. [15]
	120	2.2723(3)	2.3599(6)	3.86(2)	9.56(2)	−5.70(1)	this work
800	180	1.0672(3)	1.050(2)	−1.6	9.1	−10.7	Ref. [15]
	180	1.0668(2)	1.0494(2)	−1.63(2)	9.18(2)	−10.81(1)	this work
1000	120	1.9273(5)	2.027(4)	5.2	5.8	−0.6	Ref. [15]
	120	1.9271(3)	2.0252(5)	5.09(2)	5.78(2)	−0.70(1)	this work
1000	180	1.1040(3)	1.098(2)	−0.5	4.4	−4.9	Ref. [15]
	180	1.1039(2)	1.0972(3)	−0.61(2)	4.41(2)	−5.00(1)	this work

the relative corrections. Ours are larger by about 4% at $\sqrt{s} = 2$ TeV and smaller by about 5% for the selected cross section close to threshold.

Finally, we have also compared the electroweak $\mathcal{O}(\alpha)$ corrections with Ref. [15], where also the $\alpha(0)$-scheme has been used. In Table 3 we list the results of Table 2 of Ref. [15] and the separate relative photonic and weak corrections of Table 3 of that paper together with the corresponding results from our Monte Carlo generator. Again the numbers in parentheses give the errors in the last digits. We reproduce the results for the lowest-order cross section within the integration errors, which are about $2–3 \times 10^{-4}$. The results for the cross section including electroweak corrections coincide to better than 0.1% which is of the order of the integration error of the results of Ref. [15]. The relative electroweak, weak, and photonic corrections agree also within 0.1%. This holds as well for the QCD corrections (not shown in Table 3).

5. Summary

We have presented results from a calculation of electroweak radiative corrections to the process $e^+e^- \to t\bar{t}H$, which is important for a precise determination of the top–Higgs Yukawa coupling. In detail, we have discussed the impact of photonic corrections at and beyond $\mathcal{O}(\alpha)$, the genuine weak $\mathcal{O}(\alpha)$ corrections, and the $\mathcal{O}(\alpha_s)$ QCD corrections.

The photonic and weak corrections both reach the order of $\sim 10\%$ and show characteristic dependences on the Higgs-boson mass and on the scattering energy. Owing to a phase-space effect the (negative) photonic corrections reduce the cross section more and more when the threshold is approached, i.e., with increasing Higgs-boson masses. Close to threshold the resummation of the higher-order ISR corrections becomes mandatory. The weak corrections, which depend on the Higgs-boson masses only moderately, range from about $+15\%$ at a CM energy of 500 GeV to about -10% at 1.5 TeV. There are large cancellations between photonic and weak corrections, and the final size of the corrections depends strongly on the input-parameter scheme. These results clearly demonstrate the necessity to include the electroweak corrections in predictions adequate for a future high-luminosity e^+e^- collider.

We have compared our results with those of other groups. The QCD corrections have been successfully checked against previous calculations. The electroweak corrections agree well with the results of the recent calculation [15] but are at variance with the results of Ref. [14] at high energies and close to threshold.

References

[1] J.F. Gunion, B. Grzadkowski, X.G. He, Phys. Rev. Lett. 77 (1996) 5172, hep-ph/9605326.

[2] H. Baer, S. Dawson, L. Reina, Phys. Rev. D 61 (2000) 013002, hep-ph/9906419;
A. Juste, G. Merino, hep-ph/9910301.

[3] M. Battaglia, K. Desch, hep-ph/0101165;
M. Battaglia, K. Desch, LC-PHSM-2001-053.

[4] T. Han, T. Huang, Z.H. Lin, J.X. Wang, X. Zhang, Phys. Rev. D 61 (2000) 015006, hep-ph/9908236.

[5] S. Moretti, Phys. Lett. B 452 (1999) 338, hep-ph/9902214.

[6] K.J. Gaemers, G.J. Gounaris, Phys. Lett. B 77 (1978) 379;
A. Djouadi, J. Kalinowski, P.M. Zerwas, Mod. Phys. Lett. A 7 (1992) 1765;
A. Djouadi, J. Kalinowski, P.M. Zerwas, Z. Phys. C 54 (1992) 255.

[7] S. Dawson, L. Reina, Phys. Rev. D 57 (1998) 5851, hep-ph/9712400.

[8] S. Dittmaier, M. Krämer, Y. Liao, M. Spira, P.M. Zerwas, Phys. Lett. B 441 (1998) 383, hep-ph/9808433.

[9] S. Dawson, L. Reina, Phys. Rev. D 59 (1999) 054012, hep-ph/9808443.

[10] S. Dawson, L. Reina, Phys. Rev. D 60 (1999) 015003, hep-ph/9812488.

[11] S. Dittmaier, M. Krämer, Y. Liao, M. Spira, P.M. Zerwas, Phys. Lett. B 478 (2000) 247, hep-ph/0002035.

[12] S. Zhu, hep-ph/0212273.

[13] S. Dittmaier, M. Krämer, M. Spira, P.M. Zerwas, LC-TH-2001-069.

[14] Y. You, et al., hep-ph/0306036.

[15] G. Bélanger, et al., hep-ph/0307029.

[16] A. Denner, S. Dittmaier, M. Roth, M.M. Weber, Phys. Lett. B 560 (2003) 196, hep-ph/0301189;
A. Denner, S. Dittmaier, M. Roth, M.M. Weber, Nucl. Phys. B 660 (2003) 289, hep-ph/0302198.

[17] A. Denner, Fortschr. Phys. 41 (1993) 307.

[18] A. Denner, S. Dittmaier, G. Weiglein, Nucl. Phys. B 440 (1995) 95, hep-ph/9410338.

[19] G. Passarino, M. Veltman, Nucl. Phys. B 160 (1979) 151.

[20] G. 't Hooft, M. Veltman, Nucl. Phys. B 153 (1979) 365;
W. Beenakker, A. Denner, Nucl. Phys. B 338 (1990) 349.

[21] A. Denner, S. Dittmaier, Nucl. Phys. B 658 (2003) 175, hep-ph/0212259.

[22] J. Küblbeck, M. Böhm, A. Denner, Comput. Phys. Commun. 60 (1990) 165;
H. Eck, J. Küblbeck, Guide to FEYNARTS 1.0, University of Würzburg, 1992.

[23] T. Hahn, Comput. Phys. Commun. 140 (2001) 418, hep-ph/0012260.

[24] T. Hahn, M. Perez-Victoria, Comput. Phys. Commun. 118 (1999) 153, hep-ph/9807565;
T. Hahn, Nucl. Phys. B (Proc. Suppl.) 89 (2000) 231, hep-ph/0005029.

[25] S. Dittmaier, Phys. Rev. D 59 (1999) 016007, hep-ph/9805445.

[26] T. Stelzer, W.F. Long, Comput. Phys. Commun. 81 (1994) 357, hep-ph/9401258;
H. Murayama, I. Watanabe, K. Hagiwara, KEK-91-11.

[27] S. Dittmaier, Nucl. Phys. B 565 (2000) 69, hep-ph/9904440.

[28] W. Beenakker, et al., in: G. Altarelli, T. Sjöstrand, F. Zwirner (Eds.), Physics at LEP2, Report CERN 96-01, Geneva, 1996, Vol. 1, p. 79, hep-ph/9602351.

[29] M. Roth, Ph.D. Thesis, ETH Zürich No. 13363, 1999, hep-ph/0008033.

[30] A. Denner, S. Dittmaier, M. Roth, D. Wackeroth, Nucl. Phys. B 560 (1999) 33, hep-ph/9904472.

[31] S. Dittmaier, M. Roth, Nucl. Phys. B 642 (2002) 307, hep-ph/0206070.

[32] G.P. Lepage, J. Comput. Phys. 27 (1978) 192;
G.P. Lepage, CLNS-80/447.

[33] Particle Data Group Collaboration, K. Hagiwara, et al., Phys. Rev. D 66 (2002) 010001.

[34] F. Jegerlehner, hep-ph/0105283.

[35] J. Fleischer, F. Jegerlehner, Nucl. Phys. B 216 (1983) 469;
B.A. Kniehl, Z. Phys. C 55 (1992) 605;
A. Denner, J. Küblbeck, R. Mertig, M. Böhm, Z. Phys. C 56 (1992) 261.